Available online at www.sciencedirect.com

ScienceDirect

Procedia Engineering 10 (2011) 1491–1496

Engineering Procedia

Experimental characterization of short fatigue crack kinetics in an austeno-ferritic duplex steel

I. Alvarez-Armas[a*], H. Knobbe[b], M.C. Marinelli[a,c], M. Balbi[a], S. Hereñú[a], U. Krupp[c]

[a]*Instituo de Física Rosario – CONICET, Universidad Nacional de Rosario, Argentina*
[b]*Institut für Werkstofftechnik, Universität Siegen, Germany*
[c]*Faculty of Engineering and Computer Science, University of Applied Sciences Osnabrück, Germany*

Abstract

The present work reports the damage evolution during low (LCF) and high (HCF) cycle fatigue behavior in an embrittled duplex stainless steel type DIN 1.4462. For LCF, the results have shown microcracks nucleating mainly along the most favorable oriented slip planes regarding the Schmid factor in the ferrite and propagating along similar planes. Occasionally, they nucleate at α-α grain boundaries. For these cracks, phase boundaries seem to be an effective barrier against the propagation in contrast to grain boundaries. During HCF, cracks initiate at α-α grain or at α-γ phase boundaries and propagate in an intercrystalline mode and propagate in the neighbor grain. LCF and HCF characteristics have been related to the associated dislocation structure and with the local crystallography obtained by EBSD analysis in order to understand the propagation behavior.

Selection and peer-review under responsibility of ICM11

Keywords: LCF; HCF; Duplex stainless steels; embrittlement; microstructure; EBSD techniques; microcrack nucleation and propagation.

1. Introduction

When high strength and excellent corrosion resistance are required, duplex stainless steels are the selected family of steels. Many applications imply cyclic loading and thus the knowledge of fatigue

* Corresponding author: e-*mail*: alvarez@ifir-conicet.gov.ar

Selection and peer-review under responsibility of ICM11 doi:10.1016/j.proeng.2011.04.249

damage is an important parameter to be considered for dimensioning. However, these grades of steels embrittle when exposed in the temperature range of 280-500ºC limiting their application to temperatures below 280ºC. The occurrence of the 475°C embrittlement in the ferrite is due to the presence of a miscibility gap in the Fe-Cr system, which decomposes into α (Fe-rich) and α' (Cr-rich) phases developing an internal stress field responsible for strengthening of the alloy. The main drawback of the embrittlement is that it changes the tensile, fracture and fatigue behavior of this steel.

Most dimensioning strategies make use of the fatigue limit, which is based on the assumption that below a certain stress value no cycle-dependent damage occurs. However, recent investigations have shown that metallic structures may fail beyond the conventional fatigue limit. It is postulated by several authors that once slip bands are formed, cyclic slip irreversibility causes fatigue failure sooner or later. However, Krupp et al [1] have found that standard duplex stainless steel exhibits at least a technical fatigue limit up to $N = 10^8$ cycles since phase boundaries were identified as effective barriers against slip transfer. In the embrittled material, the information about cyclic behavior is very scarce. Recently, it was reported that the embrittlement in modern duplex stainless steel seems not to have a detrimental effect concerning fatigue life in the elasto-plastic range [2, 3]. Regarding LCF, microcracks initiate with a very high density firstly in the embrittled ferrite and propagate along slip markings in the austenite. On the other hand, during high cycle fatigue [4], an embrittled standard DSS shows pronounced slip bands in the austenite, which develop marked extrusions where cracks initiate, while the aged ferrite hardly shows traces of damage. This fact has been attributed to a consequence of the higher cyclic yield stress of the spinodally decomposed ferrite which might require a higher applied stress for plastic deformation leaving the austenite as the only phase that sustains plastic strain within the HCF regime.

In the annealed material during LCF, although the cyclic plastic activity begins firstly in the austenite and then continues to the ferrite, a strong relief is developed rapidly in the ferrite. Consequently, microcracks initiate preferentially at α/α grain boundaries and then propagate along slip markings formed successively in the austenitic and ferritic grains [5]. Krupp et al [6] have determined that the propagation rate depends on the elasto-plastic behavior of each phase, the misorientation angle between slip bands of neighboring grains and the barrier strengths of the different types of boundaries.

The aim of this study is to analyze the cyclic and microstructural behavior including microcrack nucleation and propagation of the embrittled standard DSS during low and high cycle fatigue in order to correlate the transition from one range to the other.

2. Experimental procedure

The behavior of microstructurally short fatigue cracks was studied in an austeno-ferritic duplex stainless steel DIN 1.4462. The chemical composition of the material is: C: 0.02; Cr: 21.9; Ni: 5.6; Mo: 3.1; Mn: 1.8; N: 0.19; P: 0.023; S: 0.002; Fe balance. After a 4 hours homogenization heat treatment at 1250ºC followed by slow-cooling to 1050ºC and quenching in water, the microstructure consists of approximately 50% austenite with a mean grain size of 30 μm embedded in 50% ferrite with a mean grain size of 27 μm, Fig 1 a). Finally, the material was aged at 475ºC during 100hs, resulting in Vickers hardness values of (HV 0.05, 10 sec) 254 HV in the austenite and 465 HV in the ferrite.

Cylindrical shallow notched specimens for low cycle fatigue (LCF) [3] and high cycle fatigue (HCF) [7] were manufactured. The notch focuses the fatigue damage in the zone of observation. Prior to testing, the specimens were ground and electro-polished to eliminate any roughness. The central part of the notch for LCF was monitored during the test using a powerful optical system consisting of a CCD camera JAI mod. For HCF, the test area of the shallow notch was studied by direct observation in real time using a long-distance QUESTAR optical microscope coupled to a digital camera.

Push-pull LCF tests were performed at room temperature on an electromechanic testing machine. The tests were carried out under plastic strain control with a fully reversed triangular wave at constant total strain amplitude of 0.3% and total strain rate of 2 $x10^{-3}$ s^{-1}. In order to record the surface damage, the test was stopped (at 80% of σ_{Max}) periodically. Push-pull HCF tests were carried out in a servohydraulic testing system under stress control, σ=400 MPa, stress ratio R =-1 and frequency f=10 Hz. Rotational bending fatigue tests have been also carried out to compare the fatigue life of specimens in the annealed and embrittled condition. Internal dislocation structures were studied in thin foils taken from slices cut at different depths, parallel to the specimen axis, from the shallow-notched area of the specimen on the side opposite the dominant crack.

3. Results and discussion

Figure 1 a) shows the microstructure of the aged material before testing and b) and c) the surface damage after the LCF test at rupture. Figure 1 b) depicts the damage distribution consisting of slip lines and microcracks observed by secondary electron contrast and Fig. 1 c) represents the superposition of secondary and backscattered electron contrast in order to visualize only the microcracks (encircled). The austenite activates at least 2 or 3 slip systems homogeneously distributed while the ferrite can activate more than one in a grain but the deformation is localized heterogeneously in the grain. The microcracks initiate in the ferrite even though the deformation initiates in the austenite and is much more pronounced than in the ferrite.

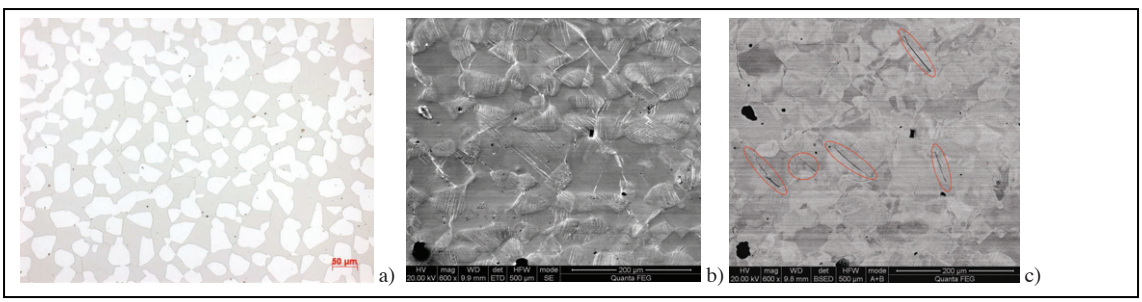

Fig. 1: a) Microstructure of the aged material before being tested; b) and c) surface damage on the notched area of the specimen after the LCF test carried out at $\Delta\varepsilon_p$=0.003 at rupture (see description in the text)

Table 1 summarizes the behavior of the microcracks of Fig. 1 b) and c) in detail. The important result is that microcracks initiate in crystallographic planes with the highest SF in the ferrite and propagate also along crystallographic planes with the highest Schmid factor (SF) even in the neighbor grain. It is interesting to note that most of these planes are of the {112} family.

Figure 2 shows the crack growth of cracks 2 and 4 according to the table and the SEM images when propagating into the austenitic phase. These diagrams reveal that the propagation rate in the ferritic grain is very fast; namely only in few cycles are needed. The embrittled phase needs low energy to let a nucleated crack propagate along a crystallographic plane. Then, at the phase boundary, crack 2 reduces the growth rate and continues in the austenitic phase with a lower growth rate. At this stage, it does not achieve to propagate along a slip plane in the austenite. As is shown in Fig. 2 c), the crack exhibits a zigzag behavior near the interphase boundary. In the other case, crack 4 is arrested during several cycles at the phase boundary, Fig. 2 b), and then continues with a similar crack growth rate as crack 2 and propagates along a crystallographic plane following the data of Table 1.

Contrary to what happens in the nucleation and propagation of microcracks in the DSS in the as-received condition [5, 8], the activation of the slip systems in the ferrite phase is controlled by the SF.

Table 1: Crystallography of short crack nucleation and propagation during LCF. *PhB: phase boundary

Crack	initiation and propagation in the same grain: {hkl} ; SF	propagation in neighbor grains: *ibid*	propagation: *ibid*
#1	PhB* in {110} ; 0.41 → {112} ; 0.27 → {112} ; 0.46 (secondary cracks in {112} ; 0.49)	{111} ; 0.44	
#2	{112} ; 0.49	zig zag interphase	
#3	PhB in {112} ; 0.47 → {112} ; 0.46	zig zag interphase → {111} ; 0.44	
#4	{112} ; 0.49	{111} ; 0.43	
#5	{112} ; 0.49		
#6	PhB in {112} ; 0.45	{111} ; 0.45	
#7	α-α grains	{110} ; 0.49	upper {111} ; 0.43 lower {111} ; 0.42

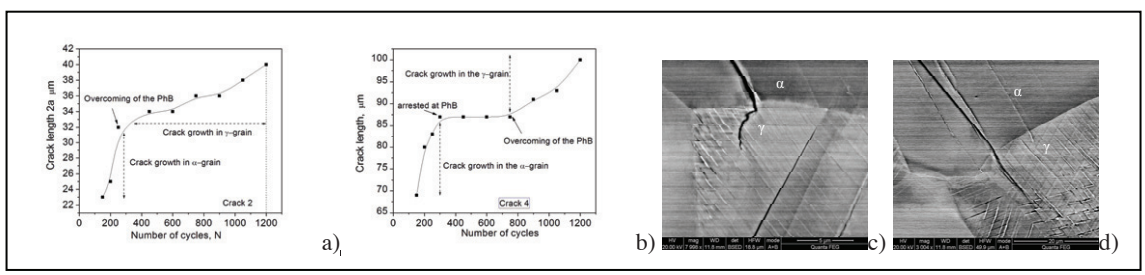

Fig. 2: Crack growth behavior during LCF: a) crack 2; b) crack 4 from Table 1. SEM micrographs of the overcoming α-γ in: c) crack 2 and d) crack 4.

Results of rotating bending fatigue tests have revealed that the embrittled condition does not affect the fatigue life of the steel. The examination of the specimen surface during the HCF test shows different features due to the cyclic plastic deformation process. The first slip markings appear in the austenitic phase and in a few ferritic grains. As cycling proceeds, slip lines in the austenitic phase intensify and propagate into the neighboring ferritic grains while slip lines nucleated in the ferritic phase propagate into the neighboring ferritic grains or remain arrested at the α-γ phase boundary. Concerning microcrack initiation, three different situations have been observed: i) nucleation in α-α boundary and propagation along the grain boundary up to the next α-γ boundary; ii) nucleation in α-γ boundary and propagation in the α-grain up to the next barrier and iii) less common, nucleation along slip planes in α-grains.

Figure 3 a) shows the aspect of the surface damage after HCF. Figure 3b) and c) represent the behavior of a single crack nucleated at an α-α boundary propagating into the austenitic grains and the corresponding crack growth curve. In this graph, it is marked different stage of the microcrack growth, namely, the microcrack initiation at a ferritic grain boundary, the arrest at the phase boundary and the growth in the austenitic grains. As in the LCF results, phase boundaries represent a solid barrier to crack propagation. The barrier effect of phase boundaries is generally higher than the grain boundaries irrespective of the angles between possible slip systems in the adjacent grains [6].

TEM observations in LCF specimens have revealed a strong activity in the austenitic grains. Most of them present the usual planar arrangement of dislocations in two or three slip systems. However, many other grains show a transition to a more developed structure, Fig. 4 a). The ferritic grains confine the

dislocations in one or two slip plane depending on the SF, leading to a low dislocation density in the rest of the grain, Fig. 4b). The activated slip planes are heterogeneously distributed inside the ferritic grains. In agreement to the EBSD data, it corresponds to the activation of the most favorable slip planes either {110} or {112} or in both if the SF is favorable to slip. The α' regions exert a restraining effect on dislocation motion owing to their different lattice parameter, among other factors, are consequently responsible for hardening and embrittling the microstructure [9].

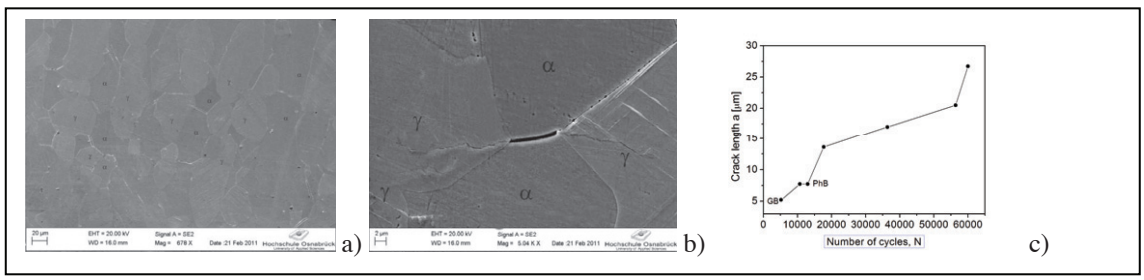

Fig. 3: a) Surface damage in the HCF regime; b) microcrack nucleated at α-γ boundary; c) crack growth curve

The behavior of the microcrack growth during propagation through a ferritic grain and the corresponding overcoming of a phase boundary as presented in Fig. 2 can be rationalized as follows. Due to the restraining effects that exerts α' zones on dislocations motion, the ferrite grains are not capable to accumulate too much plastic strain during fatigue. Thus, once the activated slip planes fulfill the capacity to deform plastically, microcracks nucleate on them. On the other hand, the ductility of the austenitic grains permits dislocation to accommodate in more complicated structures for longer time. Therefore, when a microcrack arrives from a ferritic grain at the phase boundary, it remains arrested until the adjacent zone in the neighboring austenitic grain hardens due to strain localization. Consequently, a loss of ductility is produced in this area or eventually in the whole grain and the crack is able to surpass the boundary and propagate in the neighboring grain.

The dislocation structure in HCF is pretty different. The austenitic phase activates one slip system Fig. 4 c) and the ferritic phase shows scarcely plastic activity. The most deformed ferritic grains present a homogeneous distribution of dislocations, Fig. 4 d). According to this scenario, the plastic activity developed in the γ grains and the crystallographic mismatch between the α-γ grains involved (based on the KS relation) are two necessary conditions to the generation of high rugged areas near the interfaces, and therefore to a preferential site for crack nucleation at the phase boundaries in fatigued DSS [10].

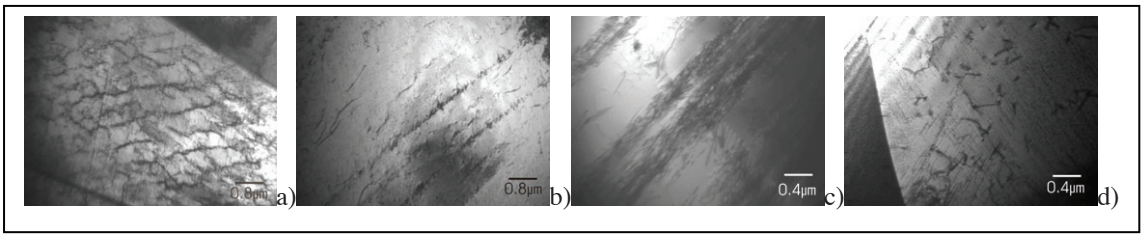

Fig. 4: Dislocation structure. After LCF: a) near-cellular arrangement in the austenite; b) dislocation slip band in the ferrite. After HCF: c) band structure in the austenite; d) homogeneous dislocation distribution in the ferrite.

Concerning the nucleation at α-α grain boundary, where the plastic activity in both ferritic grains is barely present, high incompatibility stresses due to the elastic anisotropy can contribute to crack initiation. This phenomenon is well known and was investigated in the context of twin-boundaries in austenitic steels by several authors [11,12].

4. Conclusions

The analysis of the damage evolution during LCF and HCF behavior in an embrittled duplex stainless steel type DIN 1.4462 have shown that: i) microcracks nucleate at α-α and α-γ boundaries during HCF while during LCF they nucleate mostly along slip planes favorably oriented for slip in the ferrite; ii) α-γ phase boundaries are strong barriers to crack propagation during both LCF and HCF, namely, the ductile austenite has the capacity to accumulate plastic deformation and thus, it delays the formation of the favorable conditions to allow crack propagation.

Acknowledgements

This work was supported by Alexander von Humboldt Foundation, Agencia Nacional para la Promoción de la Ciencia, Técnica and Consejo Nacional de Investigaciones Cientícas y Técnicas (CONICET) and by the cooperation program DAAD/MinCyT between Germany and Argentina.

References

[1] Krupp U, Knobbe H, Christ HJ, Köster P, Fritzen CP. The significance of microstructural barriers during fatigue of a duplex steel in the high- and very-high-cycle-fatigue regime. *Int J Fatigue* 2000; **32**:914-20.

[2] Armas AF, Hereñú S, Alvarez-Armas I, Degallaix S, Condó A, Lovey F. The influence of temperature on the cyclic behavior of aged and unaged super duplex stainless steels. *Mater Sc. Eng A* 2008; **491**:434-39.

[3] Balbi M, Avalos M, El Bartali A, Alvarez-Armas I. Microcrack growth and fatigue behavior of a duplex stainless steel. Int J Fatigue 2009; **31**:2006-13.

[4] Llanes L, Mateo A, Violan P, Mendez J, Anglada M. On the high cycle fatigue behavior of duplex stainless steels: Influence of thermal aging, *Mater Si. Eng. A,* 1997; **234-236**:850-52.

[5] Marinelli MC, El Bartali A, Signorelli JW, Evrard P, Aubin V, Alvarez-Armas I, Degallaix-Moreuil S. Activated slip systems and microcrack path in LCF of a duplex stainless steel. *Mater Sci Eng A* 2009; **509**:81-88.

[6] Krupp U, Düber O, Christ HJ, Künkler B, Schick A, Fritzen CP. Application of the EBSD technique to describe the initiation and growth behavior of microstructurally short fatigue cracks in a duplex steel. *J of Microscopy* 2004; **213**:313-20.

[7] Düber O, Künkler B, Krupp U, Christ HJ, Fritzen CP, Experimental characterization and two-dimensional simulation of short-crack propagation in an austenitic–ferritic duplex steel. *Int J Fatigue* 2006; **28**:983-92.

[8] El Bartali A, Aubin V, Degallaix S. Surface observation and measureme nt techniques to study the fatigue damage micromechanisms in a duplex stainless steel. *Int. J. Fatigue* 2009; **31, 11**:2049-55.

[9] P J. Grobner, The 475°C embrittlement of ferritic stainless steels, *Metal. Trans.* 1973; **4**:251-60

[10] Vogt JB. The fatigue properties of Duplex Stainless Steels: role of microstructure. *Key Eng Mat* 2008; **378-379**:101-14.

[11] Heinz A, Neumann P. Crack initiation during high cycle fatigue of an austenitic steel. *Acta Metall Mater* 1990; **38,10** :1933-40.

[12] Blochwitz C, Tirschler W. Influence of texture on twin boundary cracks in fatigued austenitic stainless steel. *Mater Sci Eng A* 2003; **339**:318-27.